Sodium Laser Guide Star Brightness, Spotsize, and Sodium Layer Abundance

Jian Ge[a], B.D. Jacobsen[a], J.R.P. Angel[a], P.C. McGuire[a],, T. Roberts[a], B. McLeod[b]
M. Lloyd-Hart[a], D. Sandler[a,c]

[a]Steward Observatory, The University of Arizona, Tucson, AZ 85721, USA

[b]Center for Astrophysics, MS 20, 60 Garden Street, Cambridge, MA 02138, USA

[c]ThermoTrex Corporation, 10455 Pacific Center Court, San Diego, CA 92121, USA

ABSTRACT

We report on new results of simultaneous measurements of sodium layer abundance and the absolute return flux from laser guide stars created by a monochromatic 1 W cw laser, tuned to the peak of the sodium D2 hyperfine structure. The return was conducted at the MMT and the sodium abundance was measured at the CFA 60 inch telescope, about 1 km away from the MMT, with the Advanced Fiber Optic Echelle (AFOE) spectrograph. The laser frequency stability, which can greatly affect the return flux, was monitored at the same time in order to improve the measurement accuracy. After the correction of laser frequency jitter and atmospheric transmission, the absolute flux return for circularly polarized light is 1.71×10^6 photons s^{-1} m^{-2} per watt launched, per unit column density, which we take as our measured mean over the year of N(Na) = 3.7×10^9 cm^{-2} at Tucson. The solidification of a final well-determined relationship between the sodium laser guide star brightness and sodium layer column density is pivotal in the design of the next generation laser guide star adaptive optics systems.

We also report the measurements and analysis of the relationship between the projected beam waist of the sodium laser and the resultant spot size on the sodium layer under typical atmospheric conditions. Knowledge of the waist size is crucial to the design of the laser beam projector for optimal performance. By projecting the laser through diffraction limited optics of roughly 3 r_0 diameter, we have achieved the smallest artificial beacon yet recorded, about 0.8 arcsec.

Keywords: Adaptive Optics, Laser Guide Star, Sodium Layer Abundance, Point Spread Function

1. INTRODUCTION

Adaptive optics (AO) systems can significantly reduce atmospheric distortion effects in astronomical imaging if a bright light source is available within arcmin field-of-view of a scientific object for measuring wavefront phase errors. However, the sky coverage for the AO systems relied on natural bright field stars is only a few percentage of the sky (e.g. Roddier 1995). In order to significantly increase the sky coverage with AO correction, laser-generated artificial guide stars or "beacons" are required for sensing the wavefront errors (e.g. Sandler et al. 1994). The most promising artificial laser guide star is generated by focusing a sodium laser beam tuned to the sodium D_2 line at 589 nm on the mesosphere sodium layer at about 90 km altitude.

Several groups in the world have begun to explore the use of sodium laser guide star technique for astronomical adaptive optics (e.g. Jacobsen et al. 1993; Max et al. 1994; Jelonek et al. 1994; Avicola et al. 1994). In the Fall 1996, our group successfully closed the laser guide star adaptive optics tip-tilt system loop resulting in the first reported improvements in image quality (Lloyd-Hart et al. 1997). In early 1997, Livermore laser guide star group also successfully closed their high order AO loop and made significant image corrections (Olivier et al. 1997). The recent closed loop experiments with sodium laser guide stars at Max-Plank-Institut fur Astronomie have also demonstrated a factor of two image improvements in the near-IR (Hippler et al. 1998). These experiments demonstrate the possibility of sodium laser guide star technique in adaptive optics applications. However, there is as yet no consensus on the optimum laser and power. The choice depends not only on the laser power, but also on

Other author information: (Send correspondence to Jian Ge)
J. G.: Email: jge@as.arizona.edu; WWW: http://qso.as.arizona.edu/~jge; Telephone: 520-621-6535; Fax: 520-621-1532

the inherently different pulse formats and frequency purity of different laser types. Theoretical calculations predict differences in return for the same power and column density up to a factor 5 according to pulse format (Milonni & Telle, 1996, private communication), but these have yet to be confirmed experimentally. Thus, experiments that measure column density and details of the excitation and scattering properties of sodium atoms in the sodium layer are very important to refine the design parameters of the laser and assess the power requirement.

Simultaneous local observations of the sodium column density and the laser return are necessary to obtain the fundamental relationship between the magnitude of the laser guide star and sodium abundance. Previous studies have shown that the column density of the sodium layer varies with time, including long term seasonal variations and short term variations (e.g. Papen 1996; Ge et al. 1997), and also varies with latitude (Hunten 1966; Magie et al. 1978; Papen et al. 1996; Ge et al. 1997). A simultaneous measurement of column density and guide star brightness has not been done before. This together with the measurements of sodium layer abundance variation (Ge et al. 1997) will provide a reference for the design of the sodium laser for the MMT 6.5 m AO system as well as other sodium AO systems in the world.

In order to obtain the strongest signal from a sodium laser guide star for wavefront sensing and correcting, the images at a Shack-Hartmann wavefront sensor should be as sharp as possible. A doubling of the image would require a quadrupling of laser power to obtain the same signal/noise ratio (e.g. Sandler et al. 1994). The instantaneous spot size on the sodium layer is directly related to the sodium laser beam waist size. The optimal sodium laser beam waist width varies with the instantaneous atmospheric conditions. Therefore, a series of experiments need to be conducted to find out the relationship between the optimal sodium beam waist and spot size and how tight a spot the laser beam projector generates on the sky.

In this paper we will report on simultaneous sodium laser return and mesosphere sodium abundance measurements, instantaneous sodium beam waist width and spot size measurements.

2. SIMULTANEOUS SODIUM LASER RETURN AND COLUMN DENSITY MEASUREMENTS

The most proper way to determine how much laser power is required for certain laser guide star AO performance is to directly calibrate the laser power with the simultaneous measurements of sodium laser guide star flux and sodium layer abundance. The continuous-wave dye laser we used for the MMT FASTRAC II AO system can provide a single longitudinal mode with tunable frequency at high powers after it passes through a traveling-wave ring cavity and frequency tuning elements (Roberts et al. 1997). It is perhaps the simplest laser for the simultaneous measurements. The observational results can be easily understood and provide a good reference for predicting other laser guide star performance. Furthermore, the results provide a direct testing of current theoretical models for sodium laser guide stars (Milloni & Telle 1997, private communications).

The simultaneous measurements of sodium laser return flux and mesosphere sodium abundance were conducted in March, May, and September, 1997. The sodium laser return flux was measured at the Multiple Mirror Telescope (MMT) on Mt. Hopkins. The laser output power was measured before and after each collecting data set with typical 10 image frames, which were typically taken in totally about 3 minutes. The exposure time of each frame is 3-5 seconds. The average laser power projected on the sky is about 1 watts for the all three runs. Only the sodium return flux during photometric conditions were used for the final data analysis. In fact, during each return experiment the laser beacon images were used for choosing those photometric measurements because any thin clouds passing through the laser beams would show very strong Rayleigh scattering and significantly reduce the return flux from the sodium spot. Especially during the September run, because thin clouds covered part of the sky, we took advantage of the laser beacon high sensitivity to thin clouds to use the laser return images to help find clear sky patch for the return measurement.

The sodium layer abundance was measured at the CFA 60 inch telecope with the Advanced Fiber Optic Echelle (AFOE) spectrograph. The telescope is only about 1 km away from the MMT on the same mountain. Therefore, similar sodium layer patches were observed by both telescopes. The specrograph resolving power is R = 50,000 (Brown et al. 1994). With such spectral resolution, the sodium D_2 line is blended with telluric water absorption lines, the D_1 absorption line, which is clearly separated from other nearby telluric absorption lines, is therfore the only suitable line for the sodium abundance measurements. Because the very weak telluric sodium D_1 absorption line

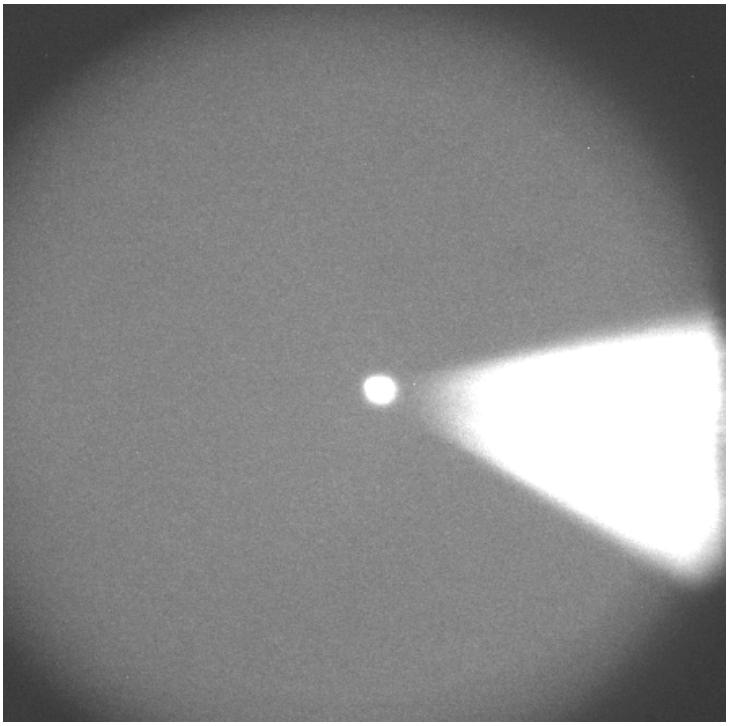

Figure 1. Typical image frame of the sodium resonant fluorescence recorded at the MMT with an Apogee CCD camera for the simultaneous sodium laser return measurements. The dimension of the frame is 140x140 arcsec^2.

could be easily buried in much stronger interstellar D_1 absorption lines and/or stellar D_1 absorption itself from late type stars, only a couple of very nearby early type stars without interstellar or stellar D_1 absorption are suitable for the measurements. About a dozen of nearby bright early type stars with magnitude brighter than 3 magnitude have been searched by us to find suitable targets for this project. So far only four such stars were found, and they are α Leo, α Aql, β Tau and α And. However, the number of stars suitable for the measurements will increase once higher resolution spectra are obtained because higher resolution will help to separate telluric D_1 line from other interstellar D_1 lines (cf. Welty et al. 1994) and also stellar D_1 line becomes much broader than the telluric D_1 line.

Because the equivalent width of typical telluric sodium D_1 absorption line is less than 1 mÅ, in order to measure the sodium abundance to better than 15% error, a signal-to-noise ratio (S/N) of at least 1,000 is required for spectral resolution R $\sim$ 50,000. With 16 bit CCD readout electronics, a S/N of $\sim$ 500 can be reached in each frame. On the other hand, once the S/N reaches about 500, CCD pixel-to-pixel variation will limit improvements in S/N. To solve this problem, we coadded $\sim$ 100 flat frames, which were taken a few hours before or after the simultaneous experiments for accurately tracing the CCD pixel sensitivity variation, and divided the combined object frames (α Leo in the March run, and α Aql in the May run and the September run) by the combined flat. The resulting S/N can reach as high as $\sim$ 2,000, which is good enough for accurate sodium abundance measurements.

Figure 1 shows the typical image of the sodium resonant fluorescence observed through one of the MMT mirror during the September run. In order to avoid possible saturation of sodium laser power on the sodium layer, we let the telescope a little out of focus to the sodium layer. The average spot size for the all three observational runs is about 3 arcsec, or about 1.3 m diameter on the sodium layer. We also pointed the telescope to the direction close to the bright stars, which were chosen for measuring the telluric sodium abundance, to sample the similar sodium layer patches.

The laser guide star and standard star images were recorded by a thermally cooled Apogee CCD camera mounted on the telescope. The data were reduced in the standard way with the IRAF package. The photometry of laser guide stars and standard starswas measured by using the IRAF package PHOT. The estimated error of the photometry is

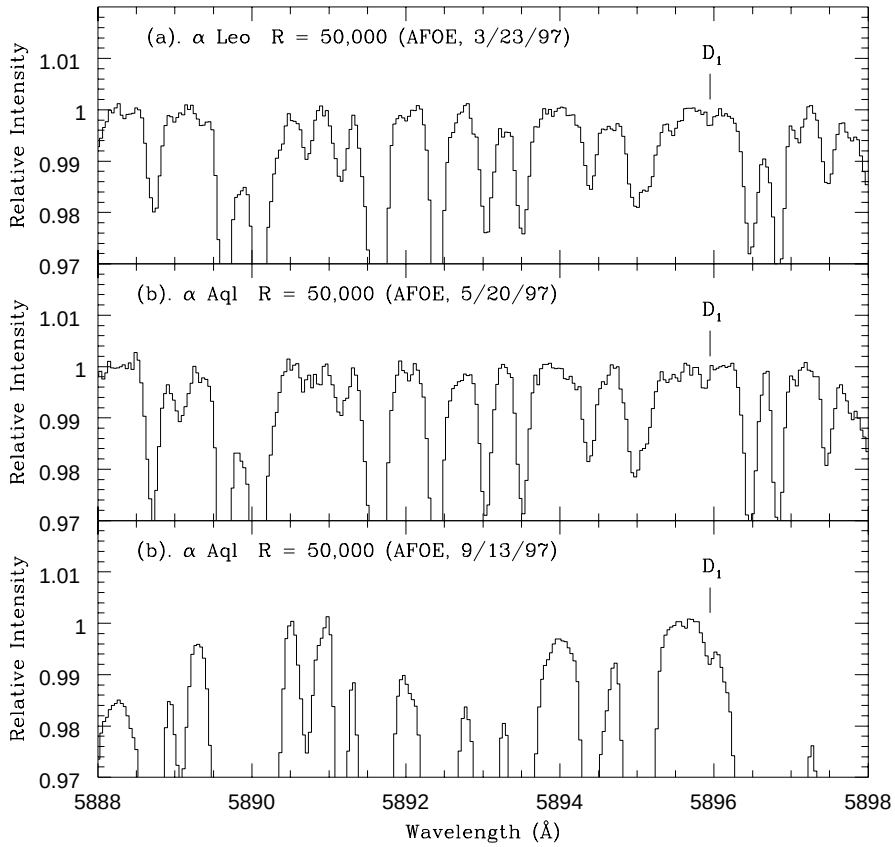

Figure 2. Typical telluric sodium D_1 absorption spectra obtained at the CFA 60 inch telescope with AFOE spectrograph and R = 50,000. The absorption lines from water vapor are much stronger for the September data than those for the March and May data.

2.5% based on the standard star flux measurements.

Figure 2 shows the typical telluric D_1 absorption spectra from the September run, as well as from previous runs. Telluric D_1 lines from the three different runs show similar line strength. However, the absorption lines from telluric water vapor are significantly different, especially those water lines from the September run are much stronger than those from the other two runs. The strong water absorption lines in the September data are almost blended with the weak D_1 line. Therefore, this figure further demonstrates that the spectral resolving power of 50,000 is a minimum requirement for accurate measurements of sodium layer column density under different weather conditions.

Previous studies show that the mesosphere sodium D_2 absorption is normally very weak, e.g. the typical optical depth at the center of the absorption line is $\tau_0 \sim 0.04 << 1$ (Ge et al. 1997; Ge, Angel & Livingston 1998), it is appropriate to assume that the D_1 absorption line, which line strength is a half of the D_2 line (Morton 1991), is in the linear portion of the curve of growth, where the column density of the atoms is proportional to the equivalent width. The integrated number of sodium atoms per square centimeter in the line of sight is then given by

$$N = 1.130 \times 10^{20} \frac{W_\lambda}{f\lambda^2}\ cm^{-2}, \tag{1}$$

where W_λ is the equivalent width, and both W_λ and λ are in unit of Å, f is the oscillator strength ($f = 0.318$ for the D_1 transition at 5895.94 Å Morton 1991). The error resulting from neglecting the saturation effect was estimated to be less than about 2.5%, which is within the measurement error of about 10% caused by the photon statistics.

The measurement results from 1997 March and May runs have been published in the workshop proceeding on Laser Technology and Laser Guide Star Adaptive Optics Astronomy (Ge et al. 1997). A strong correlation has been

found between the absolute laser guide star flux and sodium layer abundance. Further, the circularly polarized laser beam provides $\sim 30\%$ increase in fluorescent return over linearly polarized beam. The measurement errors from the column density and the guide star brightness have been found to be relatively small (e.g. $\sim 15\%$ for the sodium abundance and 3% for the photometric measurements). However, the systematic error caused by the laser itself could be very large (e.g. $\sim 50\%$). Moreover, the atmospheric transmission could also affect the absolute return flux measurements. Therefore, new sodium return experiments with simultaneous measurements of laser frequency and atmospheric transmission are required to estimate possible systematic errors in previous measurements.

During the September run, we monitored the laser frequency with a Fabry-Perot interferometer and a Edmund CCD camera. We have also measured the atmospheric transmission through observing several standard stars at different airmass during the same observation run.

Table 1 shows the measurements of simultaneous absolute return flux from linearly and circularly polarized sodium laser beams and sodium column density from the March, May and September runs, 1997, as well as the observation time and airmass and corresponding R magnitude of the laser artificial stars. The absolute sodium laser return flux is defined as the flux measured without the atmospheric transmission loss. The atmosphere transmission was $T \approx 0.9$ at the Zenith during the September observation run. The same atmosphere transmission of T = 0.9 is assumed for the March and May observation runs.

Table 1. Simultaneous Linearly and circularly Polarized Laser Return and Column Density Measurements

Polarization	Time (MT)	Airmass	Absolute Return Flux at Zenith (10^5 Photons/m^2/s/W)	N(Na) at Zenith (10^9 atoms/cm^2)	R mag./W
linear	1h13m, 3/23/97	1.16	4.0	2.2±0.5	11.4
linear	3h18m, 5/20/97	1.17	8.2	3.0±0.5	10.6
linear	3h23m, 5/20/97	1.17	11.7	4.3±0.7	10.2
linear	3h33m, 5/20/97	1.18	10.1	4.6±0.7	10.4
linear	3h39m, 5/20/97	1.18	10.6	4.3±0.7	10.3
circular	12h32m, 3/23/97	1.07	4.9	1.7±0.5	11.1
circular	1h16m, 3/23/97	1.21	4.5	2.1±0.4	11.2
circular	1h26m, 3/23/97	1.21	5.9	1.9±0.5	10.9
circular	1h55m, 3/23/97	1.28	5.7	2.7±0.4	11.0
circular	2h45m, 5/20/97	1.12	14.0	4.5±0.7	10.0
circular	3h08m, 5/20/97	1.14	11.3	3.3±0.6	10.2
circular	4h04m, 5/20/97	1.26	8.6	3.6±0.7	10.5
circular	4h08m, 5/20/97	1.26	5.8	2.7±0.5	11.0
circular	4h14m, 5/20/97	1.28	12.6	5.1±0.9	10.1
circular	4h18m, 5/20/97	1.29	13.8	5.8±0.9	10.0
circular	0h32m, 9/13/97	1.00	12.6	3.8±0.6	10.1
circular	0h49m, 9/13/97	1.41	11.5	4.6±0.7	10.2
circular	0h59m, 9/13/97	1.41	12.1	4.4±0.8	10.2
circular	1h28m, 9/13/97	1.41	12.8	3.4±0.5	10.1

Figure 3 shows the relationship between the absolute laser guide star flux and sodium abundance at the Zenith. The backscatter from circularly polarized beams obtained from three different observation runs is proportional to sodium column density. The absolute return measurements from the September run are consistent with previous ones. Figure 3 also shows theoretical prediction of the absolute laser return flux (the dashed line) based on the following estimate

$$N_r = N_t \epsilon \frac{A_c}{4\pi H^2} 1.5, \tag{2}$$

where N_r is backscatter in unit of photons s^{-1}, $N_t = 3.0 \times 10^{18}$ photons s^{-1} is the total output flux of 1 watt sodium laser, A_c is the photon collector area. $H = 90$ km is the height of the sodium layer above the telescope, $\epsilon = \sigma_P N_{Na}$,

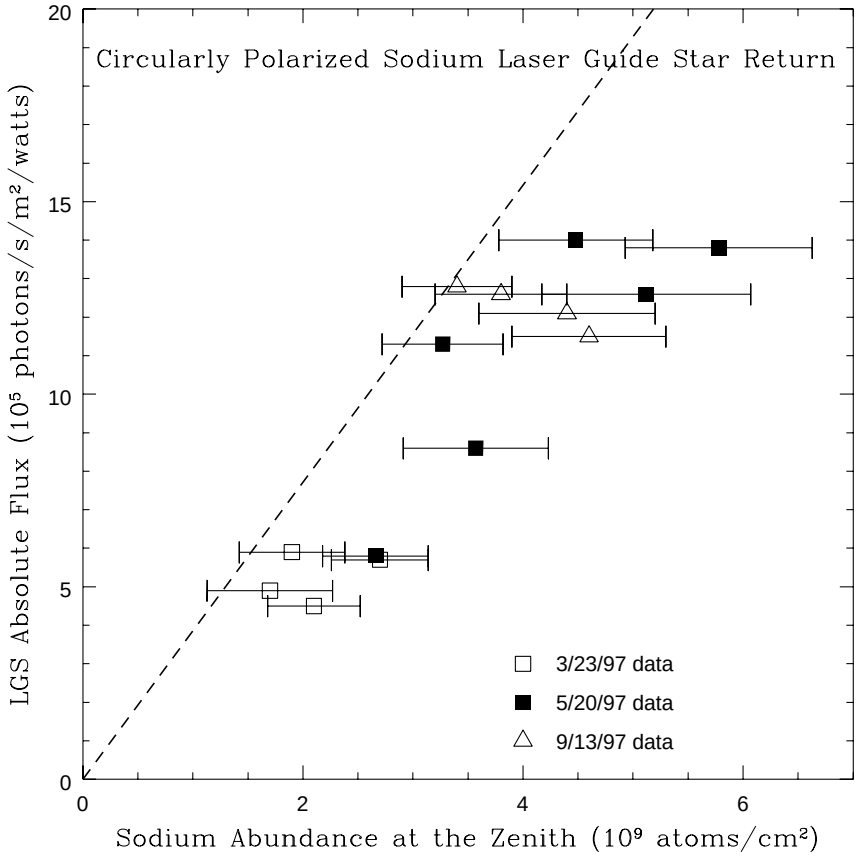

Figure 3. Absolute flux of sodium laser returns of circularly polarized beams vs sodium layer abundance at Zenith.

where N_{Na} is the sodium column density, and the peak cross section of the D_2 hyperfine $\sigma_P = 8.8 \times 10^{-12}$ cm^2 is applied because < 10 MHz line width for the cw dye laser tuned to the hyperfine peak is very narrow compared to the 1.19 GHz FWHM of the D_2 hyperfine line (Happer et al. 1994). The angular dependent scattering factor, 1.5, for the backward is also used in equation (2) (Jeys 1991). The theoretical predicted values are larger than the measured values from the circularly polarized laser beams. This result should be expected because the laser frequency was found not always locked on the frequency corresponding to the peak of the D_2 hyperfine structure, which would result in less return flux.

The laser frequency instability was monitored by a Fabry-Perot interferometer. Figure 4 shows the typical interferogram from this interferometer recorded by an Edmund CCD camera. The interferograms were recorded and used to measure the simultaneous laser frequency. We found that the laser frequency mainly hopped among four adjacent modes randomly. The frequency difference between the two neighbor modes is 0.276 GHz, which is determined by the ring laser cavity size. The laser mode hopping rate is higher than 3 Hz. Once the sodium laser mode hopped from the mode with frequency corresponding to the peak of the D_2 hyperfine structure to other modes, the return intensity should be much less because of the smaller cross-section associated with the other mode frequency (Milloni & Telle 1996). If the typical kinetic temperature of the sodium layer, T = 210 K, is assumed (Ge et al. 1997; Happer et al. 1994), then the effect sodium cross section for the September return measurements is 2/3 of the peak value.

If the correcting factor of 2/3 is applied to the September sodium return results, then a laser guide star with R = 9.8 mag. or absolute flux of 1.71×10^6 photons s^{-1} m^{-2}, is expected to be formed from 1 watt of projected circularly polarized sodium cw laser when the sodium laser frequency is locked on the peak of the D_2 hyperfine structure and the sodium layer abundance is at its mean value of N(Na) = 3.7×10^9 cm^{-2} at our latitude (Ge et al. 1997). This value is 2.0 times that we reported in our previous paper, is consistent with the prediction from theoretical studies

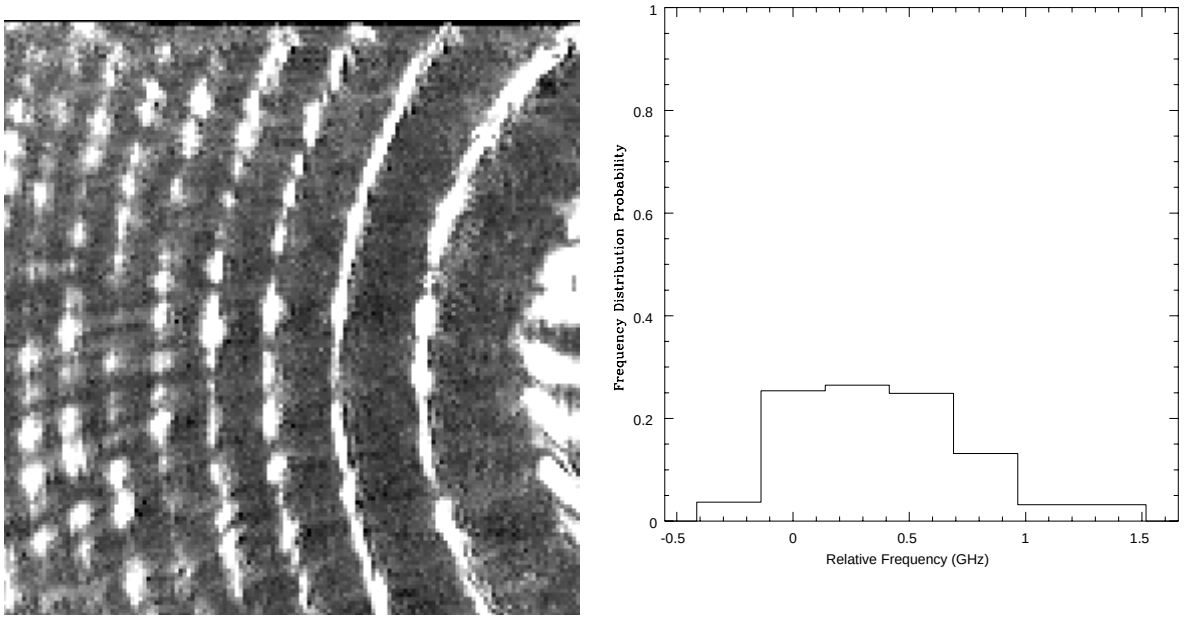

Figure 4. (a). Interferogram from a Fabry-Perot etalon to monitor laser frequency jitter during the sodium laser return experiments. (b). Laser frequency distribution function. The sodium dye laser mode separation with the ring cavity is 0.276 GHz. The zero frequency corresponds to the frequency of the peak cross-section of the sodium D_2 hyperfine structure.

including the Earth's magnetic field and optical pumping effects (Milonni 1997, private communication). The main difference between this result and previous one (Ge et al. 1997) is that we have included the correcting factor caused by the laser frequency jitter, as well as the measured atmospheric transmission into the consideration to reduce systematic errors in the final value.

The refined simultaneous measurement results provide a reliable base for the design of next generation sodium laser guide star AO systems. Based on these results, the detected sodium laser return photon number for a collecting aperture with an area of A (m^2) in the integration time τ (milliseconds) is

$$N = 1710 T^2 \tau P A \eta, \tag{3}$$

when P watts single mode sodium cw dye laser, locked to the D_2 peak cross section frequency, is launched to the sodium layer. The η is the total collecting system efficiency including sky and collecting system transmission and detector quantum efficiency. If the return photons are collected by a Shack-Hartmann wavefront sensor for wavefront correction, then the total wavefront reconstruction error for each subaperture is (see Sandler et al. 1994 for details)

$$\sigma^2_{rec} = \frac{4\pi^2 G \alpha^2}{N} (\frac{FWHM}{\lambda/d})^2 (1 + \frac{4n^2}{N}) (\frac{0.589}{\lambda})^2. \tag{4}$$

where N is the number of detected photons in each subaperture which is described in Eq. (3), $FWHM$ is the sodium spot size viewed by each subaperture, d is each subaperture size, n is the detector readout noise. Therefore, the more photons each subaperture can collect, the less the resulting wavefront reconstruction error is. On the other hand, Eq. (4) also demonstrates that the wavefront reconstruction error strongly depends on the sodium spot size. For example, a doubling of the spot size would require a quadrupling of laser power to maintain the same wavefront correcting performance. Therefore, it is very important to build a sodium laser beam projector which can provide the sodium layer spot size as small as possible.

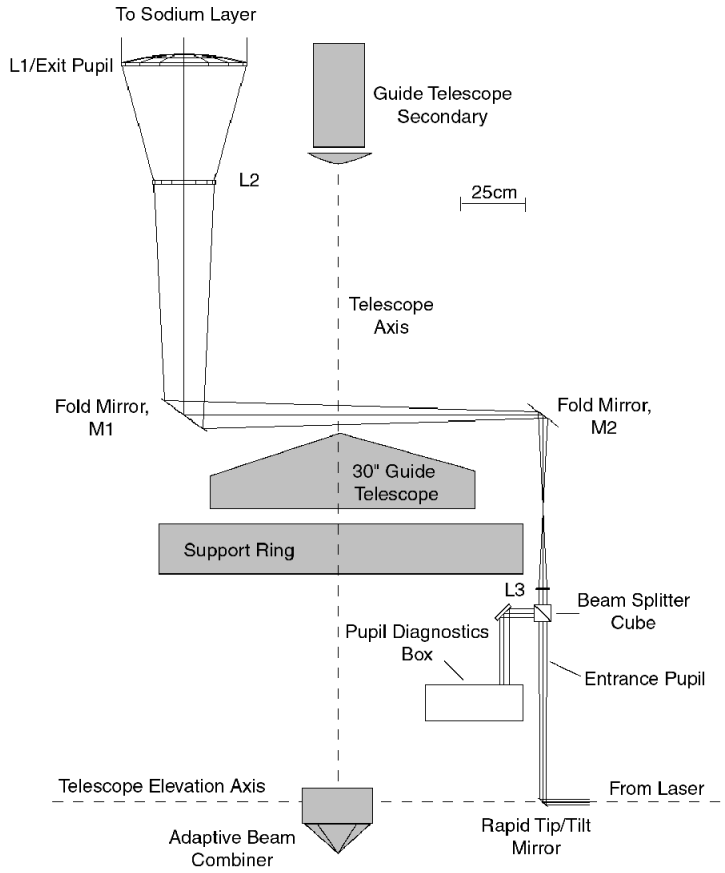

Figure 5. Diagram of the sodium laser beam projector as it was mounted on the MMT during the 1997 March, Mar and September runs.

3. SODIUM SPOT SIZE AND SODIUM BEAM WAIST MEASUREMENTS

Figure 5 shows the schematic drawing of the sodium laser beam projector, which was used for measuring the sodium beacon size and sodium waist during the September run at the MMT (Jacobsen 1997, Ph.D. dissertation for details). The top primary projector pair (PPP) is a compact telephoto design with finite conjugates. The diameters of the top plano-convex BK7 lens and the second plano-concave SF5 lens are 48 cm and 25 cm, respectively. The focus lens, L3, a 2 inch commercial achromat with a focal length of 250 mm, is located 340 cm below the PPP. Because the guide telescope secondary occupies the space on the telescope axis, the PPP had to be mounted 50cm away from the axis. In addition the guide telescope primary, its cover and support structure comprise a significant obstacle to the beam path. The light must be brought vertically from the elevation axis past the guide telescope support (Figure 5). It is in this leg that L3 and the pupil diagnostics camera suite are located. Two large mirrors mounted on rigid steel towers are used to transfer the beam around the guide telescope and its cover and into the PPP.

Below the second of these mirrors is a long optical rail mounted vertically. L3 is mounted to this optical rail. Also on this rail are two, 2 inch beam-splitter cubes used to feed a diagnostics box, and a variable iris located at the entrance pupil of the projector. A pupil diagnostics box is located next to the vertical optical rail. The cameras in this box provide real time alignment and laser quality information, and a diode provides 'power in the bucket' measurements.

Below the vertical optical rail, mounted on the elevation axis of the telescope is the rapid tip/tilt mirror, which is located 1 m below the actual entrance pupil. This leads to a small amount of cross coupling between image motion and pupil filling. The tip/tilt mirror, controlled by the wavefront sensor computer, is capable of 1arcsec motions at

a rate of nearly 700Hz. In this way the global jitter of the laser can be eliminated.

The relay system consists of a series of four mirrors that bring the laser beam from the laser room up to the elevation bearing of the telescope, then sending the beam down the elevation axis of the telescope to the rapid tip/tilt mirror. The first mirror of this relay system, the one nearest to the laser, has a slow tip/tilt capability, and is used to ensure proper pupil filling. Also included in this relay system is a remotely activated shutter connected to the electronic airplane "watching dog". This shutter is used to block the beam in case of aircraft passing near the beam.

Near the laser itself is the polarization control system and the beam expander. The polarization control consists of a MgF2 crystal with tip/tilt. The polarization control for the current system is run manually with real time feedback from the polarization detector. Also on the laser bench is a variable beam expander. The beam expander consists of two positive lenses mounted on an optical rail. By varying the spacing and slightly adjusting the focusing lens on the vertical optical rail the projected beam waist can either be varied up or down to match the projected beam waist to the optimal waist.

The performance of the current beam projector are mainly considered in two areas. The first is amount of energy transmitted from the laser to the sky, and the second is how tight a spot the projector generates on the sky.

The current projector has seven reflective surfaces and 18 refractive surfaces. Most of the mirror surfaces are coated with protected silver coatings and most of the refractive surfaces are coated with broadband coatings. When the projector was first installed on the telescope in 1995 the total system transmission was measured at between 70Since then some of the reflective surfaces have degraded significantly, specifically the large silvered mirrors on the telescope structure. In addition, the top surface of L2 has gathered a significant amount of dust. Cleaning this surface and recoating mirrors would require the removal of part of the beam projector system. Since this procedure would require several days or more of effort to replace and realign and also the whole laser system setup at the MMT is only for temporary use for the FASTRAC II AO system it has been left in its current state. As of September 1997 the total transmission, including vignetting losses, had fallen to 40

The size of the sodium beacon can be degraded by projector vibrations, atmospheric turbulence, and optical aberrations. The initial run with the projector revealed a 5 arcsec elongation due to vibration of the largest mirror in the wind. Extensive reinforcements were added throughout the system that alleviated the problem. Since then no significant degradations due to vibrations have been noted. The degradation of the spot size due to turbulence cannot be alleviated. However, the effects of turbulence can be minimized through appropriate waist size choice, but some degradation is unavoidable. This degradation masks the true performance of the optics.

In order to measure the beacon spot size it must be viewed with a telescope. This creates a further complication since turbulence in the down-coming beam will degrade the beacon image. Therefore, in order to determine the actual spot size on the sodium layer a stellar point spread function (PSF) taken simultaneously with the image of the sodium beacon is needed. This would allow the de-convolution of the PSF with the image of the beacon. To attempt this, a series of experiments were conducted at the MMT in September of 1997. The goal of these experiments was to obtain simultaneous, in-focus images of a star and the sodium beacon. The focus of the sodium beacon is about 36 mm lower than the infinity focus. Since it is vitally important that both images be in focus, an instrument called "co-focal box" was constructed for this run that can introduce 36 mm of extra path length for the light from the sodium beacon (Jacobsen 1997).

In the September run, 1997, the first half of the run was dedicated to collecting more sodium return strength data described in the previous section. During the second half of the run, a series of observations were made at the MMT to observe the correlation between the beam waist size and spot size and to obtain data on the size of the sodium spot generated by the projector, optimizing the projector for the smallest spot.

The variable beam expander was used to vary the projected waist size between approximately 19 cm and 36 cm. This range runs across the optimum for average seeing conditions at the MMT. Seven settings were used for the beam expander. The beam profile was determined by moving a photo-diode across the pupil and measuring the output as a function of location. For this purpose a wooden plate with a series of evenly spaced, pre-drilled holes was used to position the diode. From these profiles the approximate waist was determined. These values are only approximate since the flickering of the laser made accurate measurement difficult.

A series of exposures at various expander settings were then taken with a natural star in the field-of-view of the Apogee CCD camera. This was done using only mirror E, which has the best imaging quality of all the primaries.

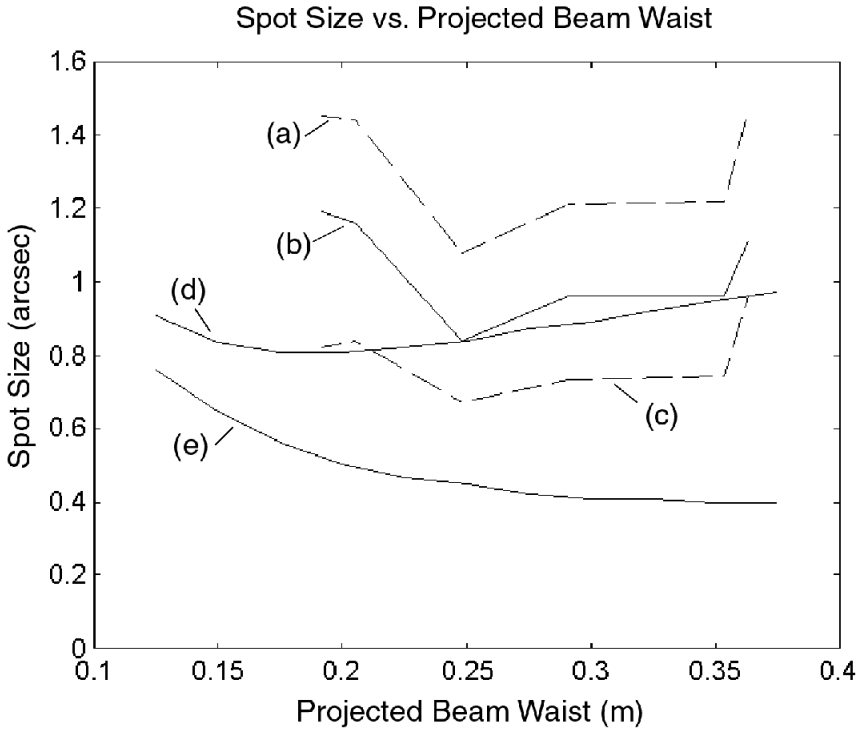

Figure 6. Comparison between the data obtained from the MMT and simulations. Curve (a) shows the average, raw image sizes of the sodium beacons for various projected waists. Curve (c) shows the average sizes of the PSF star. Curve (b) is the de-convolved spot sizes of the sodium beacons. Exposure times were between 100 and 200 ms. Curve (e) is the theoretical instantaneous spot size for $r_0 = 15$ cm measured from the PSF star images. Curve (d) is the simulated curve for a 100 ms exposure with 1.0 waves of defocus introduced into the pupil.

The exposure times were either 0.1 or 0.2 sec. The increase in exposure time was necessary to compensate for a very light, variable cloud cover, robbing the laser of power. Image sizes (FWHM) for both the star and the sodium beacon were determined by doing Gaussian profile fitting to the images using the standard IRAF package. The FWHMs of the PSF star and the sodium beacon are assumed to add in quadrature. Therefore, the actual width of the sodium beacon can be derived from the following:

$$D_{beacon} = \sqrt{(D_{image}^2 - D_{PSF}^2)}, \tag{5}$$

where D_{beacon}, D_{image} and D_{PSF} are the FWHMs of the sodium beacon, apparent sodium image and PSF, respectively.

The relationship between the waist and the beacon size did exhibit a minimum at 25 cm near the predicted optimal waist of 29 cm for average seeing conditions (Jacobsen 1997), with increased spot sizes on either side of the minimum (Figure 6). The average r_0, estimated from the instantaneous star image sizes, at the time of measurements was 15 cm. Figure 6 also shows the simulated instantaneous spot size r0 = 15 cm using the program described in Jacobsen's thesis (Jacobsen 1997). The data suggests that the beam projector was not properly optimized and that there may have been aberrations present. To simulate the effect of a simple aberration de-focus was added to the pupil. Curve (d) in Figure 6 shows simulation results for 100 ms exposures with 1 wave of defocus added to the projector. Adding the defocus drove the minimum waist size down and raised the average spot size. The minimum de-convolved spot size obtained was 0.84 arcsec which is approaching the minimum of the r0 = 10cm curve. However, this was before the optimization of the projector alignment conducted on the last night.

On the last night of the observing run several hours were spent adjusting the projector alignment while monitoring the image of the spot on the sky. This was done in an effort to truly optimize the performance of the beam projector. It was noticed at the end of this procedure that the laser beacon appeared to be strongly elongated in the direction of

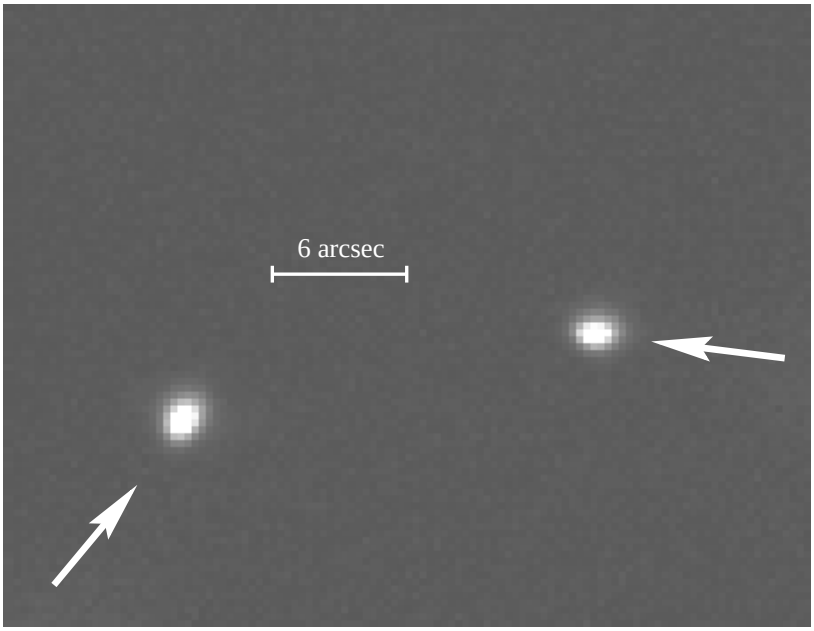

Figure 7. Sodium beacon images taken from two separate MMT mirrors. The image on the left is from mirror C and the image on the right from mirror E. The arrows indicate the direction of the Rayleigh column for the respective images, and the expected axis of radial elongation. The elongation is clearly rotated in the two images and lines up well with the expected directions. The exposure time of this frame is 0.5 s and the image size from the mirror E is 0.85 x 1.30 arcsec.

its Rayleigh column. This is the direction that one would expect to see radial elongation of the spot due to the offset of $\sim$ 2.5 m of telescope mirror E from the projector. To verify that the elongation was due to the radial offset, and not to astigmatism in the projector or imaging optics, a second mirror, mirror C, was opened as well. This mirror has a mirror-projector axis that is rotated 120° from mirror E. The subsequent image showed a clear rotation of the elongation, leading to the conclusion that the observed elongation was in fact due to the radial offset (Figure 7).

Analysis of the spot from mirror E shows a non-deconvolved spot with a major axis of 1.30 arcsec, and a minor axis of 0.85 arcsec. Additional data taken with a natural star in the field yielded an average spot size of 0.8 x 1.12 arcsec in the raw image (Figure 8). The simultaneous natural star image size (seeing size) is 0.56 arcsec. Therefore, the real sodium beacon size on the sodium layer is 0.6 x 1.0 arcsec. This represents an elongation of 0.4 arcsec, corresponding to an $\sim$ 8 km FWHM thinkness of the sodium layer. To our knowledge, this is the smallest sodium beacon ever produced.

ACKNOWLEDGEMENTS

We thank the MMT staff for their great patience and help during our FASTRAC II run, Perry Berlind and Jim Peters for helping collecting and reducing 60 inch AFOE raw data, Matt Cheselka for helping converting the vedeo tape data format to standard fits format. This work has been supported by the Air Force Office of Scientific Research under grant number F49620-94-1-0437 and F 49620-96-1-0366.

REFERENCES

Avicola, K. et al. 1994, JOSA, 11, 825
Brown, T.M. et al. 1994, PASP, 106, 1285
Ge, J. et al. 1997, in ESO Workshop on Laser Technology and Laser Guide Star for Adaptive Optics, in press

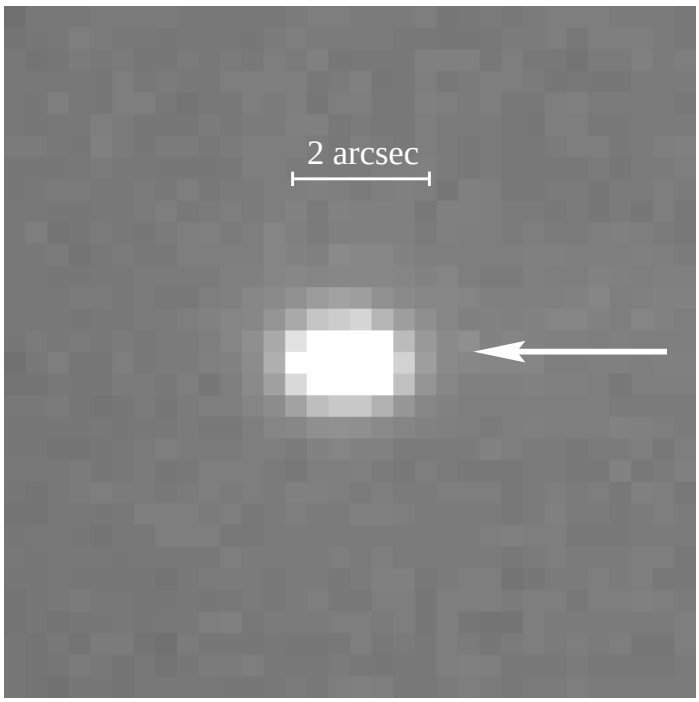

Figure 8. The image of the smallest sodium beacon recorded at the MMT when seeing is 0.56 arcsec. It is obtained from averaging 5 frames with each exposure time of 1 sec. The apparent image size is 0.8 x 1.0 arcsec. The real beacon size after deconvolution is 0.6 x 1.0 arcsec. The arrow indicates the direction of the Rayleigh scattering.

Ge, J., Angel, R. & Livingston, W. 1998, in preparation
Happer, W., MacDonald, G.J., Max, C.E., & Dyson, F.J. 1994, JOSA, 11, 263
Hippler, S. et al. 1998, These proceedings
Hunten, D.M. 1967, Space Science Reviews, 6, 493
Jacobsen, B. & Angel, R., 1997, in ESO Workshop on Laser Technology and Laser Guide Star for Adaptive Optics, in press
Jelonek, M.P. et al. 1994, JOSA, 11, 806
Jeys, T.H. 1991, The Lincoln Lab. Journal, 4, 133
Lloyd-Hart, M. et al. 1997, ApJ, 493, L950
Max, C.E. et al. 1994, JOSA, 11, 813
Magie, G. et al. 1978, Planet. Space Sci. 26, 27
Milonni, P.W., & Telle, J.M. 1997, private communications
Milonni, P.W., Fugate, R. Q., & Telle, J.M. 1997, in preparation
Morton, D.C. 1991, ApJS, 77, 119
Olivier, S.S. et al. 1997, SPIE, 3126, in press
Roberts, T., et al. 1997, in ESO Workshop on Laser Technology and Laser Guide Star for Adaptive Optics, in press
Rodier, F., et al. 1995, ApJ, 443, 249
Papen, G.C., Gardner, C.S. & Yu, J. 1996, in Adaptive Optics, Vol. 13, OSA Technical Digest Series (Optical Society of America, Washington DC), 96
Sandler, D.G., et al. 1994, JOSA, 11, 925